Can a Simple Two-Layer Model Capture the Structure of Easterly Waves?

Cheryl L. Lacotta

1 Introduction

Most tropical storms in the Atlantic, and even many in the eastern Pacific, are due to disturbances caused by African easterly waves. In fact, Avila [1] claims all of the 20 storms of the 1990 eastern North Pacific hurricane season can be traced back to waves originating over Africa. This connection to Africa is not always obvious as the waves seem to weaken on the eastern coast of Central America and then regenerate in the Pacific. Whether or not these disturbances propagate from Africa or develop *in situ*, the growth stage in the Pacific can often lead to a breakdown of the intertropical convergence zone (ITCZ), which in turn leads to cyclogenesis [2]. To investigate the growth of these waves in the Pacific, it would be useful to examine the progression of easterly waves from the Atlantic Ocean, over the North American continent, and into the Pacific Ocean. Unfortunately, a large data void in the eastern Pacific makes such an investigation difficult.

Another approach is to study these waves using a mathematical model. This paper proposes to simulate the structure of easterly waves using the simplest model possible: a two layer, quasi-geostrophic, linearized model. In this way, we may analyze the wave characteristics to examine the behavior of the wave as it passes from the Atlantic to the Pacific Ocean.

The second section of this paper describes the known properties of easterly waves. The third section explains and derives the model used in this investigation. A complete look at the dispersion relationship for the model is contained in the fourth section. Finally, an explanation of the results and avenues for future work are presented.

2 Characteristics of Easterly Waves

African easterly waves are westward-propagating waves originating in northern Africa from mid-June to early October. According to Burpee [3], the preferred region of origin is between 5°E and 35°E, near 15°N. Based on satellite pictures and statistical methods, Burpee dismissed orographic forcing and afternoon convection as the origin of easterly waves. Instead, he deduced that the waves are caused by an instability of the mid-tropospheric easterly jet. Specifically, the horizontal and vertical shear of the mean zonal flow may be acting as sources of energy for the African easterly waves. Burpee showed that the jet satisfies the Charney and Stern [4] instability criterion, and that these waves are thus growing both barotropically and baroclinically.

Reed and Recker [5] sketched the complete structure of easterly waves from a statistical standpoint. Their results were based on a compositing technique which yielded average properties of the 18 disturbances they studied from stations within the area defined by $130 \,^{\circ}$ E to $175 \,^{\circ}$ E, and $0 \,^{\circ}$ N to $20 \,^{\circ}$ N. In [5, Fig. 3] (this, and all other figures from [5] are shown in the appendix), the wind profiles for three of these stations are shown. The stations at Koror and Majuro represent the western and eastern ends of the network, respectively. The profile for Koror shows westerly winds below 600 mb, and easterly winds above. At the eastern end, the winds are easterly at all heights, with wind speeds increasing with height. This figure also shows that the average wave velocity is westward at 9 m/s in the eastern half of the region. In other words, they identified an interval of about 3800 km between successive ridge positions, with a ridge passing a station roughly every five days.

[5, Fig. 4] shows the composite diagram of the meridional wind speed with reference to the trough and ridge of the wave. There is a low-level maximum of northerly wind to the west of the trough, and a maximum of the southerly wind to the east. The centers of the maxima are located at about 700 mb. In comparison to these low-level winds, the upper winds are almost completely out of phase. The peak southerly winds in the upper layer are situated almost directly above the lower layer peak northerly winds, and vice versa. Vertically there is an eastward tilt between the centers of northerly and southerly wind maxima. In fact, it was observed that the maximum southerly wind at high levels lags the low-level northerly wind peak by approximately one-eighth of a wavelength.

A composite diagram of horizontal divergence [5, Fig. 8a] shows a region of convergence centered at the trough. The peak of this convergence region tilts eastward with height, just as did the maxima of the north and south winds in [5, Fig. 4]. Sitting atop this region is one of divergence, centered at about 175 mb. The altitude of this divergence suggests that it may be an effect of the spreading of cumulonimbus anvils. Consistent with the conservation of mass, Reed and Recker showed that low-level convergence forced rising motion above the trough in a composite diagram of vertical velocities [5, Fig. 8b].

The composite diagram of relative humidity [5, Fig. 6] also demonstrates the eastward tilt of the other figures. The moist air, because of the tilt, is found in advance of the trough at the lowest levels and to the rear at higher levels. The driest air follows the passage of the ridge. This is consistent with the rainfall plots of all the stations [5, Fig. 11]. When plotted as a function of wave position, the majority of the rain precedes or is coincident with the trough axis. When viewed in conjunction with [5, Fig. 8b], it appears that convection provides positive feedback to the rising motion above the trough.

3 The Model

This paper attempts to further the understanding of easterly waves through an investigation of the dispersion relationship for the two-layer, linearized, quasi-geostrophic Rossby wave equations. These equations were chosen because Holton [6] has shown that easterly waves may be theoretically interpreted as forced equatorial waves. The top and bottom layers are labelled Layer 1 and Layer 2, respectively. The equations are (after Salmon [7]):

$$\left(\frac{\partial}{\partial t} + U\frac{\partial}{\partial x}\right) \left(\frac{\partial^2 \psi_1}{\partial x^2}\right) + \beta \frac{\partial \psi_1}{\partial x} - \frac{f_0}{\delta p}\omega = 0 \tag{1}$$

$$\left(\frac{\partial}{\partial t} - U\frac{\partial}{\partial x}\right) \left(\frac{\partial^2 \psi_2}{\partial x^2}\right) + \beta \frac{\partial \psi_2}{\partial x} + \frac{f_0}{\delta p}\omega = 0$$
(2)

$$\frac{\partial}{\partial t} \left(\psi_1 - \psi_2 \right) - U \frac{\partial}{\partial x} \left(\psi_1 + \psi_2 \right) - \frac{R}{f_0} Q = \frac{\sigma \delta p}{f_0} \omega \tag{3}$$

where U is the mean thermal wind, or wind shear, in the center of mass frame of reference, ψ_1 and ψ_2 are the corresponding streamfunctions for the top and bottom layers, $\beta = \frac{df}{dy}$ where f is the Coriolis parameter, δp is the change in pressure from Layer 1 to Layer 2, R is the gas constant for dry air, and Q is a heat source. In equation (3), σ is the static stability parameter defined by $\sigma \equiv -RT_0p^{-1}d\ln\theta_0/dp$, where θ_0 is the potential temperature corresponding to the basic state temperature T_0 , and ω is the vertical velocity in pressure coordinates. With a few definitions,

$$\lambda^2 = \frac{f_0^2}{\sigma \delta p^2}, \qquad \psi = \frac{\psi_1 + \psi_2}{2}, \qquad \tau = \frac{\psi_1 - \psi_2}{2}, \qquad Q' = \frac{R}{2f_0}Q \tag{4}$$

we may eliminate ω to create a system of two equations for the two variables, ψ and τ .

$$\frac{\partial}{\partial t} \left(\frac{\partial^2 \psi}{\partial x^2} \right) + \beta \frac{\partial \psi}{\partial x} + U \frac{\partial}{\partial x} \left(\frac{\partial^2 \tau}{\partial x^2} \right) = 0 \tag{5}$$

$$\frac{\partial}{\partial t} \left(\frac{\partial^2 \tau}{\partial x^2} \right) + \beta \frac{\partial \tau}{\partial x} + U \frac{\partial}{\partial x} \left(\frac{\partial^2 \psi}{\partial x^2} \right) - 2\lambda^2 \left(\frac{\partial \tau}{\partial t} + U \frac{\partial \psi}{\partial x} + Q' \right) = 0 \tag{6}$$

The heat source term is proportional to the lower-level streamfunction. Therefore we may write $Q' = \alpha \psi_2 = \alpha (\psi - \tau)$, where α is a complex constant. Specifically α is assumed to have the form $\alpha = |\alpha|e^{i\phi}$, where $|\alpha|$ is the magnitude of α and ϕ is the phase. Based on the observations of Reed and Recker, we may choose at what phase to add the heat source term. From [5, Fig. 11] we see that most of the rainfall and cloud cover occurs over the trough axis. That implies that there must be convection at or near the trough axis. In order to have convection, a parcel must be warmer than its environment. Therefore, we need to add the heat source at a point where the lower-level environment is coolest. This results in choosing that Q' be 180° out of phase with the lower-level streamfunction, so $\alpha = |\alpha|e^{i\pi}$, or $\alpha = -|\alpha|$. For simplicity, I will write $Q' = -\alpha(\psi - \tau)$.

Assuming solutions of the form

$$\psi = Ae^{ik(x-ct)}, \qquad \tau = Be^{ik(x-ct)} \tag{7}$$

and substituting into equations (5) and (6), this system can then be written in matrix form, which after some algebraic simplifications is given by:

$$\begin{bmatrix} k^2c + \beta & -k^2U\\ (-k^2)U + 2\lambda^2U - i\frac{2\lambda^2\alpha}{k} & k^2c + \beta + 2\lambda^2 + i2\lambda^2\alpha \end{bmatrix} \begin{bmatrix} A\\ B \end{bmatrix} = \mathbf{0}$$
(8)

At this point it is useful to scale the system to a critical zonal velocity,

$$U_{crit} \equiv \beta (radius \ of \ deformation)^2 = \frac{\beta}{2\lambda^2}.$$

Then we may introduce non-dimensional parameters according to this scaling:

$$k_* = \frac{k}{\sqrt{2\lambda}}, \qquad c_* = c \frac{2\lambda^2}{\beta}, \qquad U_* = U \frac{2\lambda^2}{\beta}, \qquad \alpha_* = \alpha \frac{\lambda}{\beta}.$$

In non-dimensional terms, (8) becomes

$$\begin{bmatrix} k_*^2 c_* + 1 & -k_*^2 U_* \\ (-k_*^2) U_* + U_* - i \frac{\sqrt{2}\alpha_*}{k_*} & k_*^2 c_* + c_* + 1 + i \frac{\sqrt{2}\alpha_*}{k_*} \end{bmatrix} \begin{bmatrix} A \\ B \end{bmatrix} = \mathbf{0}$$
(9)

In order to find nontrivial solutions to the system, we must set the determinant of (9) to zero,

$$\begin{vmatrix} k_*^2 c_* + 1 & -k_*^2 U_* \\ (-k_*^2) U_* + U_* - i \frac{\sqrt{2}\alpha_*}{k_*} & k_*^2 c_* + c_* + 1 + i \frac{\sqrt{2}\alpha_*}{k_*} \end{vmatrix} = 0$$
(10)

With some algebra (and dropping the $_{\ast}$ for simplicity), we find that the dispersion relationship is:

$$c = -\frac{2k^2 + i\sqrt{2}k\alpha + 1}{2(k^4 + k^2)} \pm \left[\frac{(2k^2 + i\sqrt{2}k\alpha + 1)^2 - 4(k^4 - k^2)(1 + \frac{i\sqrt{2}\alpha}{k} + U^2k^2(1 - k^2) - i\sqrt{2}U\alpha k)}{4(k^4 + k^2)^2}\right]^{\frac{1}{2}} (11)$$

4 The Dispersion Relationship

A dispersion relationship determines the phase speed of waves of a given wavenumber. Now that we have this relationship for the model, we may investigate some special cases.

4.1 Case 1: No Heat Added

The case where there is no heating in the system provides a good check for the work done thus far. Without the α terms in (10), this case is simply the classic baroclinic instability problem. On axes of the non-dimensional wind shear and wave number, contours of the imaginary part of the phase speed, c, defined by:

$$c = \frac{-2k^2 - 1 \pm (1 + 4k^8U^2 - 4k^4U^2)^{\frac{1}{2}}}{2k^2(k^2 + 1)}$$
(12)

are plotted in Fig. 1. Shown in the plot are the contours of maximum $\Im(c)$ of the two modes. The contours of $\Im(c)$ are all positive values, implying that the wave amplitude grows for values of k and U in the contoured region. The typical textbook discussion of

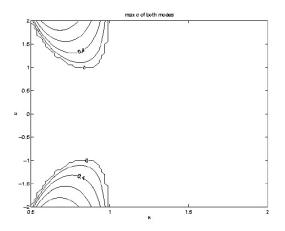


Figure 1: Contours of the imaginary part of the phase speed. No heat is added to the system.

baroclinic instability, such as that in Holton [7] shows only the upper left region of this plot. The wind shear, U, only appears as a quadratic in (12). Therefore values of $\Im(c)$ will be symmetric across the axis, U = 0. In other words, the growth of the wave has no dependence on the sign of the wind shear.

4.2 Case 2: Heat Added, No Wind Shear

As another check for the model, we consider the case in which there is no wind shear, U = 0. The heat has been added as described above. Solving for c under these conditions, we find two solutions,

$$c_1 = -\frac{1}{k^2}, \qquad c_2 = \frac{-\left(1 - \frac{i\sqrt{2\alpha}}{k}\right)}{k^2 + 1},$$

corresponding to the two possible modes of oscillation. The phase speed c_1 is simply the dispersion relationship for barotropic Rossby waves. The baroclinic mode, given by c_2 , shows wave growth for all wavenumbers. In other words, $\Im(c_2) > 0$ for all k. See Fig. 2.

The non-dimensional heating term, α , is given the value $\alpha = -1$ for this and future calculations. This was found using the scaling argument:

$$\alpha_* = \alpha \frac{\lambda}{\beta} = \frac{RQ'}{2f_0\psi_2} \frac{k}{k} \frac{\lambda}{\beta}$$
(13)

This is simply the definition of α multiplied by its scaling factor. Here, R is the gas constant, Q' is the heating rate, observed to be about 4 °C/day in the tropics, f_0 is the Coriolis parameter at about 15 °N, k is the preferred wavenumber for easterly waves, λ is the reciprocal of the radius of deformation, and $\beta = \frac{df}{dy}$ near 15 °N. The quantity ($\psi_2 k$) is merely the meridional wind speed in the lower layer, observed to be about 3 m/s. When these values are applied to (13), keeping the units consistent, we find $\alpha \sim 5$. Therefore,

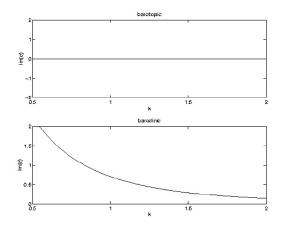


Figure 2: The imaginary part of the phase speed plotted against wavenumber for the two modes, barotropic and baroclinic, in the case without wind shear. $\alpha = -1$

 α is O(1) and must not be neglected in comparison to the other terms in (11). To be conservative, in this model we choose $|\alpha| = 1$, and considering the phase, we get $\alpha = -1$.

4.3 Case 3: Wind Shear and Heat Included

Shown in Fig. 3 are the contours of $\Im(c)$, where c is defined by equation (11).

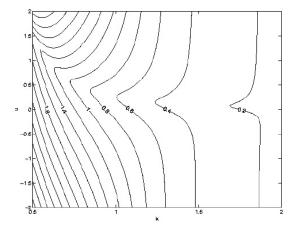


Figure 3: Contours of the imaginary part of the phase speed. Shear and heat are added.

Now, because of the heat term, the contours are no longer symmetric across U = 0. The shear term no longer appears only as a quadratic, forcing the sign of the shear to be important. Without the heat source, there are only two regions where instabilities would occur. Outside of these regions the waves are stable and will not grow. Now that heat has been added, it is clear from Figure 3 that there are no longer any stable regions. The contours of $\Im(c)$ are positive, or unstable, everywhere.

For each of the two modes, the real and imaginary parts of the phase speed have been plotted for a particular wavenumber. Recall that the non-dimensional wavenumber is defined:

$$k_* = k(radius \ of \ deformation) = \frac{k}{\sqrt{2\lambda}}$$

Since $k = 2\pi/wavelength$ by definition, we need to determine the typical wavelength of the easterly waves. Using Reed and Recker's results, we approximate the wavelength as 4000 km. With a typical radius of deformation of 1000 km for tropical waves, we find:

$$k_* = \frac{2\pi}{4000} \cdot 1000 \approx \frac{3}{2}$$

Figures 4 and 5 show the real and imaginary parts of the phase speed plotted against the wind shear for k = 1.5.

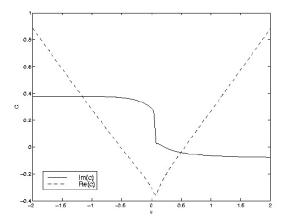


Figure 4: Contours of the real and imaginary parts of the phase speed of Mode 1. The contours are calculated for k = 1.5 and $\alpha = -1$.

Looking at the real part of the phase speed for Mode 1 (Fig. 4), we see that for small shear (|U| < 0.5), $\Re(c) < 0$, implying that the wave is easterly. However, if the shear increases, the wave becomes westerly. For this mode the wave will grow with a negative wind shear since $\Im(c) > 0$ for U < 0. By Fig. 5, however, we see that the wave will be easterly regardless of the shear in Mode 2. This is because $\Re(c) < 0$ for all U. In this mode, the wave will grow only for positive shear. Because westward propagation (characteristic of easterly waves) is independent of the wind shear in Mode 2, it seems reasonable to claim that this mode is most representative of the easterly waves studied by Reed and Recker.

To investigate this case in more detail, we will look at specific values of shear. Recall that U is defined as

$$U = \frac{U_1 - U_2}{2}$$

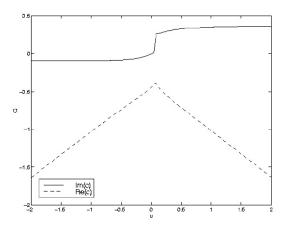


Figure 5: As in Fig. 4, for Mode 2.

where U_1 and U_2 are the zonal wind speeds for the top and bottom layers, respectively. Also recall that U was non-dimensionalized by

$$U_* = \frac{U}{U_{crit}} = U \frac{2\lambda^2}{\beta}$$

Taking U to be about 2 m/s (from [5, Fig. 3]), and U_{crit} to be about 10 m/s, we find that $U_* \approx 0.2$ m/s. Again, to be conservative in the model, $U = \pm 0.1$ was used. Referring back to Eq. (7), we set B = 1 so that

$$\tau = e^{ikx}, \qquad \psi = \frac{k^2 U}{1 + k^2 c} e^{ikx} \tag{14}$$

where c is complex. Now, using the definitions in (4), we may find the streamfunctions for the upper and lower layers. The streamfunctions for the mode with maximum growth in the case of negative shear (i.e. Mode 1 from above) are plotted in Fig. 6. The figure shows that the upper layer streamfunction is leading the lower level one by about one-eighth of the wavelength. Although the displacement between the two streamfunctions is what was observed by Reed and Recker [5], the relative placement of the two are reversed. Recall in [5, Fig. 4] that the trough axis has an eastward tilt. In other words, the lower level streamfunction should lead the upper level one.

For comparison, we now do the same analysis with the mode which has maximum growth with a positive shear, i.e. U = +0.1. The results are plotted in Fig. 7 below. Now we see that not only do we have the same displacement of one-eighth of the wavelength, but we also have the eastward tilt in the trough axis, comparable to observations of easterly waves. Once again, it appears that Mode 2 from the discussion above is representative of easterly waves.

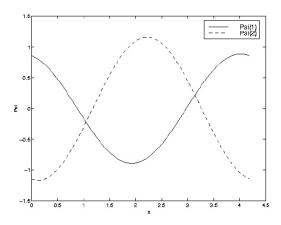


Figure 6: The upper and lower streamfunctions, ψ_1 and ψ_2 respectively, for the case of U = -0.1 and k = 1.5.

5 Conclusion

This project was developed to investigate the progression of easterly waves from the Atlantic Ocean to the East Pacific Ocean. The idea was to try to explain the wave behavior in view of a pseudomomentum argument as the wave passes the North American continent, similar to that of Held [8]. Originally, the project was to develop the relationship between the upper and lower streamfunctions, and then apply this information to the pseudomomentum theory.

The results of the model runs show that one can find a mode in the two-layer, linearized, quasi-geostrophic model that simulates the structure of easterly waves as observed in the West Pacific by Reed and Recker. The model shows an eastward tilt in the trough axis. In other words, the upper level lags the lower level. Further, the displacement between the two levels is roughly one-eighth the wavelength of the easterly wave. A more detailed analysis must be done to compare the wave speed and doubling time with observations.

In order to use this study to continue with the original research, it must be verified that the model also simulates easterly waves in the East Pacific or Atlantic Oceans. Reed and Recker's study on easterlies in the West Pacific was used only because it provided information on the complete structure of the easterlies. However, Holton [6] indicates that the shear may differ from one side of the Pacific to another. Indeed, there is variability in the shear, as evidenced by [5, Fig. 3] as one moves across the Pacific. To what extent this will affect the model has yet to be determined. Once this is known, attention may then be turned to the question of whether or not the wave behavior may be modified by pseudomomentum arguments. This is the plan for future work.

Acknowledgments I would like to thank the wonderful staff of the GFD 2000 Program, particularly my advisors for the summer: Wayne Schubert, Isaac Held, and Rick Salmon. I would also like to thank the fellows for their help, friendship, and a wonderful summer.

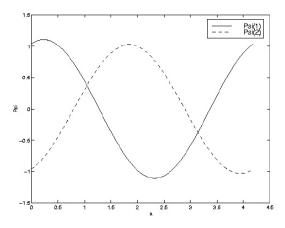


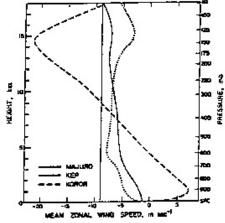
Figure 7: As in Fig. 6, for the case of U = +0.1 and k = 1.5.

References

- L. A. Avila, "Eastern north pacific hurricane season of 1990," Mon. Wea. Rev. 119, 2034 (1991).
- [2] R. N. Ferreira and W. H. Schubert, "Barotropic aspects of ITCZ breakdown," J. Atmos. Sci. 54, 261 (1997).
- [3] R. W. Burpee, "The origin and structure of easterly waves in the lower troposphere of north africa," J. Atmos. Sci. 29, 77 (1972).
- [4] J. G. Charney and M. E. Stern, "On the stability of internal baroclinic jets in a rotating atmosphere," J. Atmos. Sci. 19, 159 (1962).
- [5] R. J. Reed and E. E. Recker, "Structure and properties of synoptic-scale wave disturbances in the equatorial western pacific," J. Atmos. Sci. 28, 1117 (1971).
- [6] J. R. Holton, "A diagnostic model for equatorial wave disturbances: The role of vertical shear of the mean zonal wind," J. Atmos. Sci. 28, 55 (1971).
- [7] R. Salmon, Lectures On Geophysical Fluid Dynamics (Oxford University Press, New York, 1998).
- [8] I. M. Held and R. T. Pierrehumbert, "Dissipative destabilization of external rossby waves," J. Atmos. Sci. 43, 388 (1986).

Appendix

The following are figures taken from Reed and Recker [5].



Firs. 1. Mean model which speed for the period July-September 1967. The profile labeled KEP is the mean for Kwajakin, Enwrick and Poospe. The this vertical line denotes the average wave speed (--) m sec⁻¹) observed during the period of study.

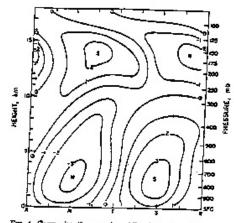
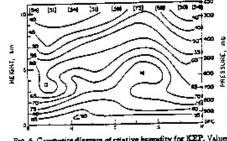


Fig. 4. Composite disgram of meridianal wind speed (m sec⁻¹) for MEP. The letters R. N. T and S refer to the ridge, north wind, though and south wind regimes, respectively, of the wave as defend by its structure in the lower troposphere.



Fro. 6. Composite diagram of relative humsdity for KEP. Values in brackets at the top are for manuration with respect to ice. Refer to Fig. 4 for further explanation.

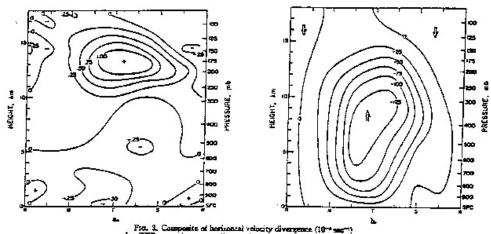
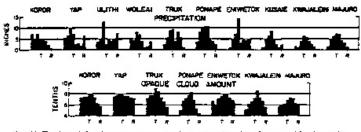


Fig. 3. Composite of horizontal velocity divergence (10⁻¹ sec⁻¹) for KEP, z., and corresponding vertical presocity (10⁻¹ mb sec⁻¹), b. (Analyzed values give approximate displacement is millbare per day.) See Fig. 4 for horizon explanation.



Fts. 11. Total rainfall and average opeque cloud amount as function of wave position for stations in the area of staty. T denotes crough axes; R, ridge axis.